Eur. Phys. J. A **20**, 59–63 (2004)
DOI 10.1140/epja/i2003-10200-6

THE EUROPEAN
PHYSICAL JOURNAL A

Gamma-ray spectroscopy studies at GANIL: Status and perspectives

G. de France[a]

GANIL, BP55027 F-14076 Caen cedex 5, France

Received: 29 January 2003 /
Published online: 9 March 2004 –

Abstract. The SPIRAL facility started to deliver radioactive beams in September 2001 and some experiments have been performed in particular using the EXOGAM array. These experiments will be briefly described and the first outputs will be shown. The in-beam performances of EXOGAM will also be discussed.

PACS. 29.30.Kv X- and γ-ray spectroscopy – 23.20.Lv γ transitions and level energies – 25.60.Pj Fusion reactions – 25.70.De Coulomb excitation

1 Introduction

The SPIRAL facility [1], producing radioactive beams at GANIL has started to deliver beams for experiments in autumn 2001, one year ago. SPIRAL uses the primary stable beams delivered by the two separated sector cyclotrons of GANIL. This high-energy, large-intensity beam is then fragmented onto a very thick carbon target producing a huge number of exotic species which are extracted from the target, selected by a low-energy separator and reinjected into a new $K = 265$ compact cyclotron (CIME). The very first beam produced and accelerated with CIME was ^{18}Ne produced by a primary beam of ^{20}Ne^{10+} at an energy of 95 A MeV. With a primary-beam intensity of 1.6 mA (300 W), the ^{18}Ne secondary beam at 7.2 MeV/A has been measured to be 10^6 pps as expected. Later on, several campaigns of radioactive-beam production have taken place. All together, 8 experiments have used ^{18}Ne, ^{6,8}He and ^{74,76}Kr: two with LISE2000 (upgrade of LISE3); three with SPEG and 4 with EXOGAM. I will concentrate on these latter ones.

In this paper, I will very briefly give the main features of EXOGAM. I will then describe the various experiments which have used SPIRAL beams and EXOGAM. It is clear that we have learnt a lot on the technical difficulties related to the setup as well as on the tricks in the analysis due to the radioactive nature of the beam and the weakness of the intensity. Because of these unusual characteristics as compared to what we were used to with stable beams, the data analysis is progressing but is not finished at all. Hence, I will limit the presentation to raw spectra which have been obtained either during the runs or shortly after. I will also discuss the limitations and describe the difficulties which came out. I will finally draw some conclusions from these first experiments.

[a] e-mail: defrance@ganil.fr

2 The EXOGAM array

A detailed presentation of the EXOGAM array can be found in ref. [2]. I will limit the spectrometer presentation to the main characteristics and sub-systems of which it is composed. EXOGAM is an array which is dedicated to study the spectroscopy of exotic nuclei and in particular using the radioactive beams from the SPIRAL facility at GANIL. This has imposed severe constraints on the design specifications: large efficiency for low and medium gamma-ray multiplicity; good signal-to-noise ratio; coupling with many auxiliary devices to cope with the various experimental conditions. These requirements end up with a design using 16 Compton-suppressed large clovers giving a photopeak efficiency of about 20% for a single gamma of $E_\gamma = 1.3$ MeV. The array (fig. 1) has a versatile geometry which allows us to have various configurations: a compact configuration (conf. A) where the detectors are located at about 11 cm from the target and a pulled-back configuration (conf. B) where the distance is 15 cm.

The four Ge crystals composing the clover are 9 cm long and have a diameter of 6 cm before shaping. They are tapered over 3 cm with an angle of 22.5 degrees. Each diode is electrically segmented into 4, in order to enhance the Doppler correction capability of the detectors.

The shield configuration is based on 3 different layers and is different in the two cases: the first one is the back-catcher in CsI; the second one, the side-catcher, is made of BGO and surrounds the rear part of the clover while the tapered length of the Ge cans is not covered; the third

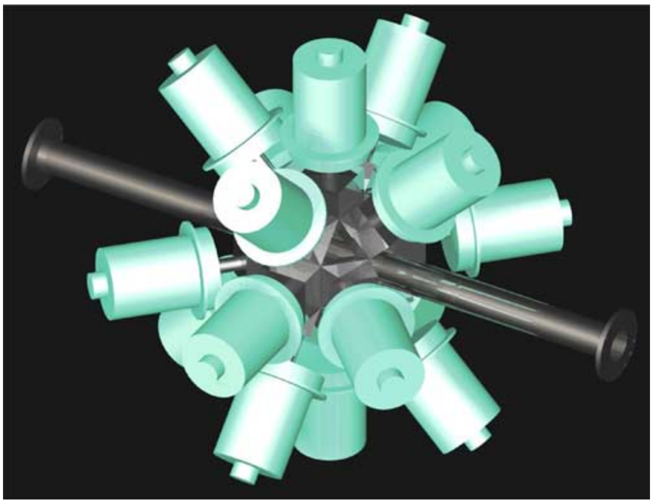

Fig. 1. Scheme of the EXOGAM array in its 16 clover configuration. The anti-Compton shields are not represented.

Table 1. Total photopeak efficiency and peak-to-total ratio calculated for EXOGAM. In configuration A, with partial Compton suppression, the 16 detectors are at 11.4 cm from the target point. In configuration B, with full suppression, the distance is 14.7 cm. The cube configuration consists in 4 clovers with full suppression at 6.8 cm from the target.

	Phot. efficiency (%)		Peak-to-total (%)	
	662 keV	1.3 MeV	662 keV	1.3 MeV
Conf. A	28	20	57	47
Conf. B	17	12	72	60
Gamma-Cube	15	10	72	60

layer, the side shield, is a long piece in BGO which covers the whole clovers starting from 2 cm before the Ge front face to the back-catcher. In conf. A, the shield consists of the two first layers: the back- and the side-catcher. The Ge are positioned in such a way that their tapered faces are in contact. This optimize the efficiency. In particular, at very low gamma ray multiplicity, it is possible to add the energy deposited in neighbouring clovers without loosing too much with pile-up effects (the *inter-clover addback*). The gain in efficiency is about 10%. When the multiplicity is larger, the detectors are pulled back in conf. B and the side shield can be mounted to significantly enhance the peak-to-total ratio. The calculated efficiencies and peak-to-total ratio are shown in table 1 for the various configurations.

The electronics is based on the VXI standard. A separate card instrument the inner (high-resolution) contact; the outer (segments with a lower resolution); and the shield. One particularity of the inner and outer contacts cards is that they contain the electronics to perform some pulse shape analysis (flash ADCs and DSPs). With the 2D segmentation, this makes of EXOGAM an excellent device to understand more in detail the gamma-ray tracking technique and possibilities.

EXOGAM will be used in coincidence with VAMOS (ref. [3]), the GANIL large solid-angle spectrometer designed for radioactive beams which is installed in another GANIL area. The coupling of the devices is made by moving the whole EXOGAM array from one room to the other with a crane. To do that, EXOGAM is mounted on a single platform on which is installed the mechanics with the detectors; the electronics in their cooled racks; the autofill, bias, and high-voltage systems for the detectors; etc. This allows to keep everything cabled between the array, the electronics and the various sub-systems.

3 Gamma-ray spectroscopy with radioactive beams from SPIRAL

3.1 Structure of excited states in heavy nuclei populated in the ^{8}He + ^{208}Pb fusion evaporation channel

The first experiment using a radioactive beam in EXOGAM has been run in April 2002 ref. [4]. The beam was ^{8}He produced by the fragmentation of ^{13}C at 75 MeV on the carbon target. The ^{8}He beam extracted from the target-source was then accelerated into CIME at an energy of 28 MeV to impinge a 30 mg cm^{-2} thick ^{208}Pb target. The beam intensity for this isotope was between 3×10^4 to 3×10^5 pps. The effective measurement time was about 58 hours before the SPIRAL target-sources broke. The failure was due to mechanical constraints within the ensemble. Since then, it has been successfully corrected. The main motivations for this experiment was to study the "high" spin states in the ^{212}Po and ^{213}At nuclei and in particular the competition between the octupole degree of freedom and the multi-particle excitations. Furthermore, and apart from the level structure studies, it was planned to measure the lifetime of the short-lived isomers in the picosecond region.

The setup for this experiment consisted in four clovers in cube geometry: three EXOGAM ones with shield plus an EUROGAM size segmented clover without shield. For the fast-timing aspect of this run, 8 small BaF2 scintillators were installed as close as possible to the target without shadowing the germanium detectors. In this geometry, the efficiency has been estimated to be 3.4% at $E_\gamma = 662$ keV. At 26 MeV, the strongest populated channel is ^{212}Po after the evaporation of 4 neutrons. As expected from the low beam intensity, the spectra obtained from this run are dominated by:

- The room background radioactivity consisting of essentially the 1461 keV line from the β-decay of ^{40}K and some decay chains from the natural Th and U isotopes. The endpoint of these decays lie in the mass region where the nuclei of interest are produced in the fusion-evaporation process.
- Beam decay: ^{8}He ($T_{1/2}$ = 119 ms) β-decays to a 1^+ state in ^{8}Li ($T_{1/2}$ = 838 ms) with a probability of 86%. The β-particle is followed by a 981 keV gamma-ray to reach the ground state. In the remaining 14% of

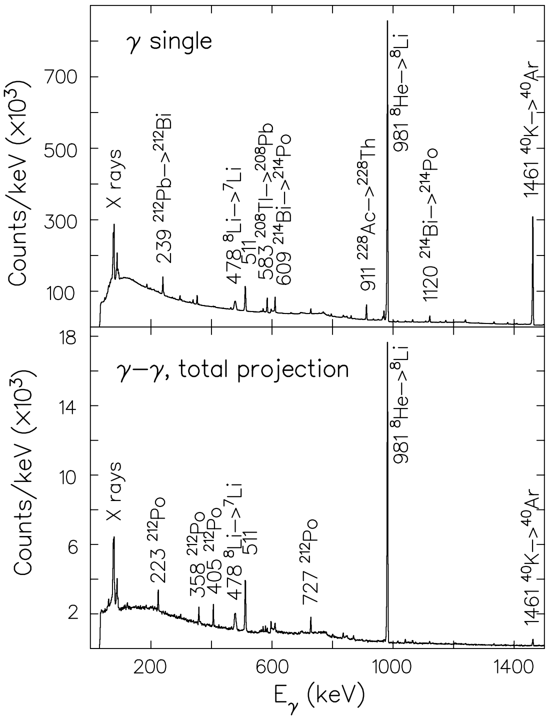

Fig. 2. Single-γ and γ-γ coincidence spectra obtained in the ^{8}He + ^{208}Pb run [4].

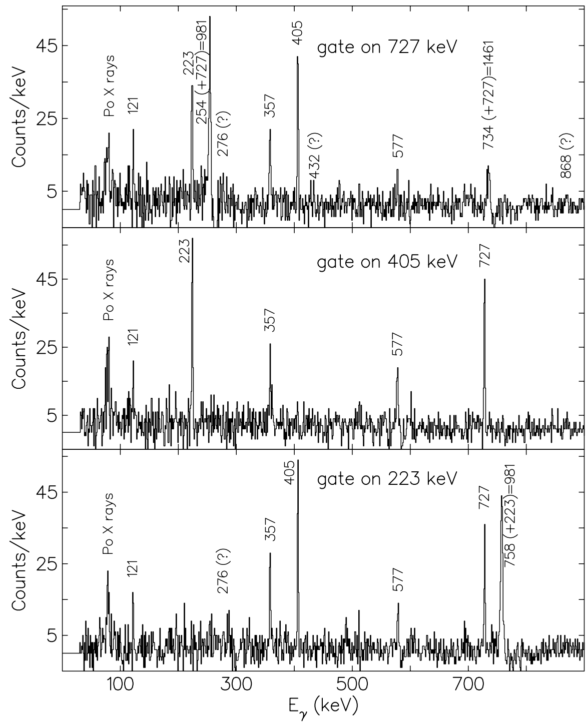

Fig. 3. Coincidence spectra obtained for ^{212}Po by gating on the $2^+ \rightarrow 0^+$ transition (top); $4^+ \rightarrow 2^+$ transition (middle) $6^+ \rightarrow 4^+$ transition (bottom) [4].

the decays, ^{8}Li emits a neutron to give ^{7}Li whose first-excited state decays via a 478 keV γ-ray. As can be seen in fig. 2, this transition is rather broad. This is due to the Doppler broadening caused by the neutron recoil.

Gamma-gamma spectra obtained by requiring the coincidence between two clovers are very different from single γ-ray spectra. However the reduction observed for most of the background (*i.e.* room background and beam decay) transitions is not seen on others. This is, for example, the case of the 1461 keV line (which is strongly reduced) and the 981 or 478 keV γ-ray which are still very strong. To understand the difference, one has to look at the details of the decay: the 1461 keV line is originating from an electron capture in ^{40}K leading to single gamma transition. The 981 keV (and also the 478 transition) follows the β^--decay of ^{8}Li and is therefore always accompanied by an electron. This latter or the brehmsstrahlung induced by its slowing-down can be detected in coincidence with the γ-ray observed in the clovers. This explains why the reduction factor resulting from the γ-γ coincidence requirement is very different. The ^{212}Po nucleus has been previously studied by A.R. Poletti *et al.* (ref. [5]). The level scheme was established up to 2.885 MeV with a tentative 14^+ spin. The gamma spectrum obtained in our case for ^{212}Po after gating on the 223 keV line (6^+ to 4^+ transition) is shown in fig. 3. With only 58 hours of beam time at this very low beam intensity (of the order of 10^5 particle per second), this spectrum shows that high-resolution gamma-ray spectroscopy is feasible.

The cross-section for elastic scattering of the ^{8}He beam is extremely large as compared to any other processes. A very simple wrapping of lead foils (for a total thickness of 9 mm) around the pipe gives a reduction of about 38% of the 981 keV line. Even if the cross-section decreases with scattering angle, the implantation of the scattered beam into the pipe, *e.g.*, is huge and must be properly shielded. An auxiliary detector must be used to go further. A first solution is to trig the acquisition system when a certain condition on the recoil products or the decaying particles is fulfilled. This possibility has been tested several times with radioactive beams and will be discussed later. When this is not easy or possible and the gamma-ray is the main trigger, another solution is to authorize the acquisition when a beam particle has been identified. This is certainly very important and can of course be combined with the previous idea. With a cyclotron RF of 11 MHz and an intensity of 10^5 particle per second, we have rougly 1 particle every 100 cycles. Combining the RF (to have an optimum time reference) and a beam detector (to trig the acquisition) would certainly improve significantly the quality of the data.

3.2 Study of very deformed ground state in neutron-deficient light rare-earth nuclei populated using ^{76}Kr beam and inverse kinematics

The second experiment using SPIRAL beams and EXOGAM was aiming at looking the very deformed ground state in the light rare-earth nuclei around ^{130}Sm. These nuclei are calculated to have a ground-state deformation of $\beta \sim 0.40$ which is equivalent to the deformation measured for superdeformed bands in the Ce region. To produce

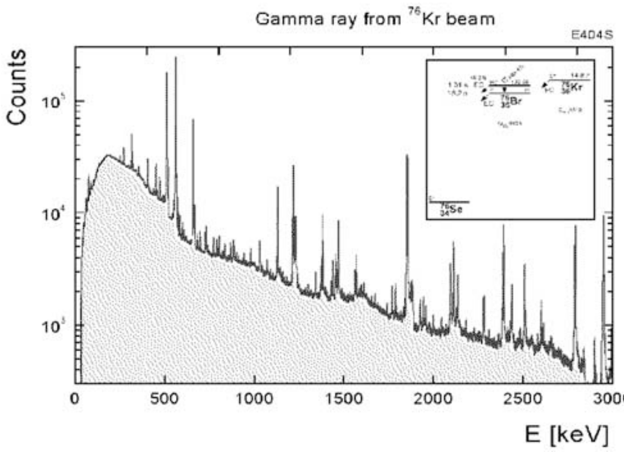

Fig. 4. Online raw spectrum obtained after $3^{h}30^{min}$ of ^{76}Kr beam time.

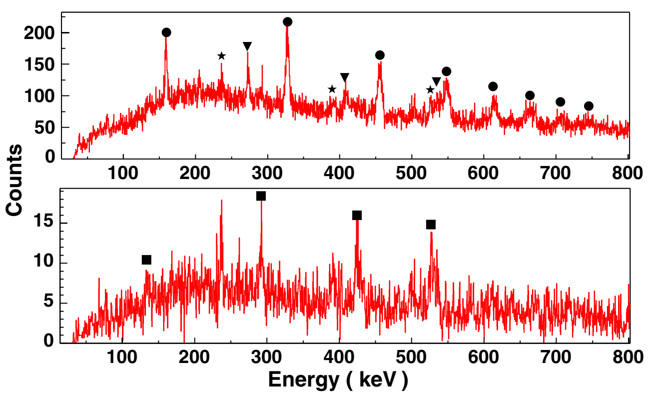

Fig. 5. γ-ray spectra obtained after demanding at least one proton (top) and at least one α (bottom) in DIAMANT. The symbols indicate γ-rays belonging to ^{130}Nd (circles), ^{131}Pm (triangles), ^{128}Nd (squares) and ^{127}Pr (stars) [6].

these isotopes, we used ^{76}Kr on a ^{58}Ni target at 350 MeV. Six EXOGAM clovers and 2 smaller ones were in the setup for this experiment which gave a photopeak efficiency of 11% at 344 keV. The DIAMANT charged-particle detector was used together with the Debrecen chessboard (both consisting in CsI detectors) to perform a better channel selection. The α and proton detection efficiency for this setup was approximately 70%. In this reaction, more than 10 channels were opened with a cross-section larger than 10 mb. An online gamma-ray spectrum corresponding to about 4 hours of beam time is shown in fig. 4.

^{76}Kr has a $T_{1/2} = 14.8$ h which builds up into the target as well as in materials which are hit by the scattered beam. Without any particle selection it is not possible to observe any γ-ray from fusion events. The particle tagging allows us to clearly identify the 4p, 3p, α2p and α3p channels leading, respectively, to ^{130}Nd, ^{131}Pm, ^{128}Nd and ^{127}Pr (see fig. 5) which are the most neutron-deficient known nuclei.

These spectra show that we have been able to observe the yrast band up to spin 18^+ in ^{130}Nd, for example. This experiment, which also had several problems related to electronics, thunderstorm, noisy DIAMANT cell, etc., has

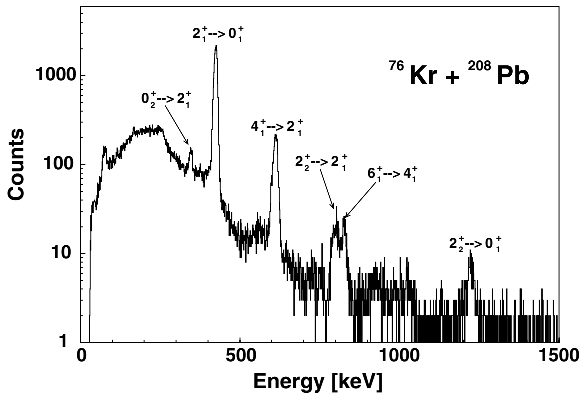

Fig. 6. Doppler corrected γ-ray spectrum obtained from ^{76}Kr Coulomb excitation on a ^{208}Pb target [7].

nevertheless shown that the coupling of these two detectors is now operational and very efficient in selecting output channels. It was already known, with stable beams induced fusion reaction, that particle identification was really efficient and required when looking for neutron-deficient nuclei. For radioactive beams this is even more critical and we observe that all the radioactivity γ-ray lines have disappeared in the α or proton gated spectra.

3.3 Shape coexistence studied by Coulomb excitation of ^{74,76}Kr beams

Following the fusion-evaporation channel, another experiment using ^{74,76}Kr radioactive isotopes took place. The goal was to study the shape coexistence in the Kr isotopes. This has been done using Coulomb excitation of the beam by various targets and at sub-Coulomb barrier incident energy. This avoids nuclear processes taking place and selects only the electromagnetic part of the interaction. The charge distribution (Q_0) is then extracted from the differential cross-section of the 2^+ state excitation probability. Several targets were used because low-lying collective states or a change in $B(E2)$ values can perturb the measurements for a single target. We used nearly the same gamma-ray setup as previously described (we had only 1 smaller detector instead of 2 for the previous one). To detect the scattered beam, an annular Si strip detector has been installed at forward angles. One of the EXOGAM triggers was conditioned by the particle detection in the Si detector. The method has the advantage to have a large reaction-section which makes it possible to run with very low beam intensity (it was down to 10^4 pps for ^{74}Kr) and low gamma-ray multiplicity. With the annular and sector segmentation of the Si detector it was possible to optimize the Doppler correction (which reach $\beta \sim 10\%$). Under these conditions, this experiment went very smoothly. In fig. 6 the online spectrum obtained with ^{76}Kr beams on the Ti target is shown. As can be seen, with the Si detector in coincidence with EXOGAM as a trigger, we obtained nearly background-free gamma-ray spectra.

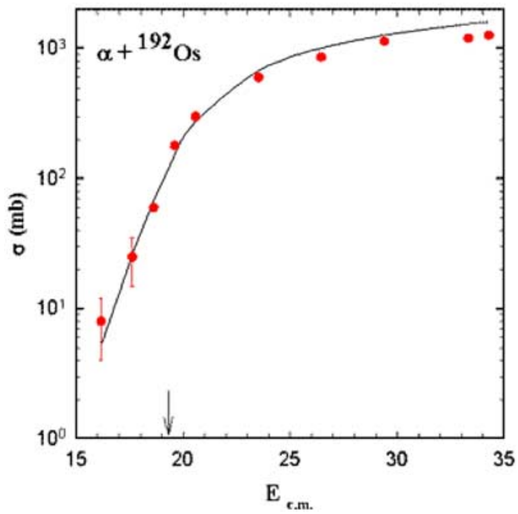

Fig. 7. Fusion cross-section for the ^{4}He + ^{192}Os measured at the BARC-TIFR pelletron at Mumbai.

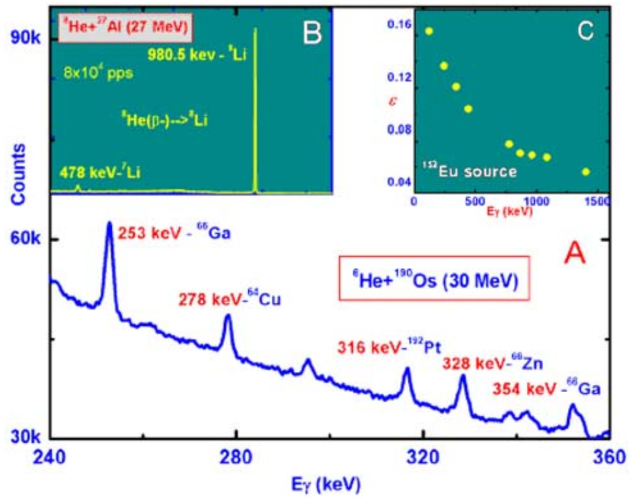

Fig. 8. Raw γ-ray spectrum obtained for the 30 MeV data (A). The γ-rays from the fusion with ^{190}Os target and the ^{63}Cu backing are identified. The insert (C) shows the total photopeak efficiency obtained for this run. The beam intensity for ^{8}He was 8×10^4 with a primary beam power of 1.2 KW at 27 MeV measured using the β-decay of ^{8}He on a thick Al target (B).

3.4 Entrance channel effect on fusion cross-section using ^{6,8}He beams

The last experiment we have made was aiming at investigating the entrance channel effects on the fusion process around the Coulomb barrier [8,9]. More precisely, the idea was to look at the effect of the loosely bound neutrons in ^{6,8}He on the fusion with different isotopes to reach the same compound nucleus. The best target-projectile couples we have found were ^{6}He + ^{190}Os and ^{8}He + ^{188}He, giving ^{196}Pt*. As a reference, we have run the α + ^{192}Os in Mumbai (India) using the TIFR-BARC pelletron Tandem accelerator at various bombarding energies. The cross-section obtained for this latter run is shown in fig. 7.

The specific difficulties of this type of measurements with SPIRAL beams are twofold: 1) measuring an excitation function with a cyclotron, and 2) precise determination of the absolute cross-section and in particular with low-intensity radioactive beams. The measurements have been done using several tools to be able to cross-check the pieces of information: highly sensitive Faraday cup, plastic detectors and annular segmented Si strip detector. For this run, the EXOGAM implementation consisted in 5 EXOGAM clovers with their anti-Compton shield and 3 smaller clovers. Again, the analysis is still going on and an online spectrum for the ^{6}He run at 30 MeV is shown in fig. 8, where the photopeak efficiency measured with a Eu source and the spectrum corresponding to the ^{8}He beam hitting an Al plate are also shown. Knowing the array efficiency and the ^{8}He decay, we estimated the beam intensity to be $i_{\mathrm{beam}} \sim 8 \times 10^4$ pps with the newly designed target-source ensemble to produce this beam.

4 Conclusions

The EXOGAM array and the SPIRAL facility have run a series of experiments during the last months. It is clear that we have learnt a lot both on the SPIRAL side and the EXOGAM one while dealing with low-intensity radioactive beams. During these runs, several auxiliary devices have been coupled to EXOGAM. This has been shown to be absolutely vital to eliminating the background. In the next coming years, the experimental programme will develop at GANIL and there is no doubt that many challenging experiments will be run and give new resuts. At the end of this paper, I want to thank the spokespersons of the experiments which I have briefly described as well as the people who worked on the data: Ph. Walker, Zs. Podolyak, N. Redon, P. Nolan, O. Stezowski, W. Korten, E. Bouchez, A. Navin, J.M. Casandjian and the numerous collaborators without whom it would have been really difficult to run the experiments. My thanks are also due to the local engineers and technicians of GANIL who worked really hard and delivered very good beams in sometime difficult conditions and also took care of EXOGAM. In particular, I am grateful to J. Ropert and G. Voltolini.

References

1. GANIL web site `http://www.ganil.fr/spiral/`.
2. GANIL web site `http://www.ganil.fr/exogam/`.
3. GANIL web site `http://www.ganil.fr/vamos/`.
4. Zs. Podolyak *et al.*, Nucl. Instrum. Methods A **511**, 354 (2003).
5. A.R. Poletti, G.D. Dracoulis, A.P. Byrne, A.E. Stuchbery, Nucl. Phys. A **473**, 595 (1987).
6. O. Stezowski, private communication.
7. E. Bouchez *et al.*, to be published.
8. V. Tripathi *et al.*, Phys. Rev. Lett. **88**, 172701 (2002) and references therein.
9. A. Navin *et al.*, private communication.